Achieving ground state and enhancing optomechanical entanglement by recovering information

2010 New J. Phys. 12 083032

(http://iopscience.iop.org/1367-2630/12/8/083032)

New Journal of Physics
The open-access journal for physics

Achieving ground state and enhancing optomechanical entanglement by recovering information

Haixing Miao[1,5], **Stefan Danilishin**[2,3], **Helge Müller-Ebhardt**[3] **and Yanbei Chen**[4]

[1] School of Physics, University of Western Australia, Perth, WA 6009, Australia
[2] Physics Faculty, Moscow State University, Moscow 119991, Russia
[3] Max-Planck Institut für Gravitationsphysik (Albert-Einstein-Institut) and Leibniz Universität Hannover, Callinstr. 38, 30167 Hannover, Germany
[4] Theoretical Astrophysics 130-33, California Institute of Technology, Pasadena, CA 91125, USA
E-mail: miah01@student.uwa.edu.au

New Journal of Physics **12** (2010) 083032 (19pp)
Received 21 March 2010
Published 12 August 2010
Online at http://www.njp.org/
doi:10.1088/1367-2630/12/8/083032

Abstract. For cavity-assisted optomechanical cooling experiments, in order to achieve the quantum ground state of the mechanical oscillator, the cavity bandwidth needs to be smaller than the mechanical frequency. In the literature, this is the so-called resolved-sideband or good-cavity limit, and this is based on an understanding of optomechanical dynamics. We provide a different but physically equivalent explanation of such a limit: that is, information loss due to finite cavity bandwidth. With an optimal feedback control to recover the information in the cavity output, we can surpass the resolved-sideband limit and achieve the quantum ground state. In addition, recovering this information can also significantly enhance the entanglement between the cavity mode and the mechanical oscillator. Especially when the environmental temperature is high, such optomechanical entanglement will either exist or vanish critically depending on whether information is recovered or not. This provides a vivid example of a quantum eraser in the optomechanical system.

[5] Author to whom any correspondence should be addressed.

Contents

1. Introduction

Recently, achieving the quantum ground state of a macroscopic mechanical oscillator has aroused great interest among physicists. It will not only have a significant impact on quantum-limited measurements [1] but also shed light on quantum entanglement involving macroscopic mechanical degrees of freedom [2]–[7], which can be useful for future quantum computing and help us to understand transitions between the classical and quantum domains [8]–[10].

By using a conventional cryogenic refrigeration, O'Connell *et al* have successfully cooled a 6 GHz micromechanical oscillator down to its quantum ground state [11]. Meanwhile, to cool larger and lower-frequency mechanical oscillators at a high environmental temperature, there have been great efforts in trying different approaches: active feedback control or parametrically coupling the oscillator to optical or electrical degrees of freedom [12]–[33]. The cooling mechanism has been discussed extensively, and certain classical and quantum limits have been derived [34]–[44]. In the case of cavity-assisted cooling schemes, pioneering theoretical works by Marquardt *et al* [36] and Wilson-Rae *et al* [37] showed that the quantum limit for the occupation number of the oscillator is $(\gamma/2\,\omega_m)^2$ (see footnote 6). Specifically, it dictates that, in order to achieve the ground state of the mechanical oscillator (i.e. with an occupation number equal to zero), the cavity bandwidth γ must be much smaller than the mechanical frequency ω_m, which is the so-called resolved-sideband or good-cavity limit. This limit is derived by analyzing the quantum fluctuation of the radiation pressure force on the mechanical oscillator. Here, we use a different but physically equivalent perspective on such a limit. It can actually be attributable to information loss: information about the oscillator motion leaks into the environment without being carefully treated, which induces decoherence.

This perspective immediately illuminates two possible approaches for surpassing the limit. (i) The *first* one is to implement the novel scheme proposed by Elste *et al* [45], in which, via destructive interference of the quantum noise, the information of the oscillator motion around ω_m does not leak into the environment. Corbitt suggested an intuitive understanding

[6] There is a factor of two difference in defining the cavity bandwidth here compared with the one defined in [36].

by thinking of an optical cavity with a movable front mirror rather than a movable end mirror in those cooling experiments [46]. In this hypothetical scheme, optical fields directly reflected and those filtered through the cavity both contain the information about the front-mirror motion. If the cavity detuning is appropriate, these two bits of information destructively interfere with each other, and the quantum coherence of the mechanical oscillator is maintained. (ii) The *second* approach is to recover the information by detecting the cavity output. This will work because the conditional quantum state—*best knowledge of the oscillator state conditional on the measurement result*—is always pure for an ideal continuous measurement with no readout loss[7]. Indeed, when the cavity bandwidth is much larger than the mechanical frequency, the cavity mode will follow the dynamics of the oscillator and can therefore be adiabatically eliminated. The quantum noise can be treated as being Markovian and a standard stochastic-master-equation (SME) analysis has already shown how the conditional quantum state approaches a pure state under a continuous measurement [47]–[51]. For a finite cavity bandwidth considered here, the cavity mode has a dynamical timescale comparable to that of the mechanical oscillator. Correspondingly, the quantum noise has correlations at different times and becomes non-Markovian. To estimate the conditional state, a Wiener-filtering approach is more transparent than the SME approach [52]. As we will show, the quantum state of the oscillator conditional on the measurement of the cavity output is indeed almost pure, with residue impurity contributed by the thermal excitation, imperfections in the detection and the optomechanical entanglement between the cavity mode and the oscillator.

Since generally the conditional mean of the position and momentum of the oscillator is non-zero, the conditional quantum state is a coherent state. In order to localize the oscillator in the phase space and achieve its ground state, we need to remove the conditional mean of the position and momentum by using a feedback control. Depending on the feedback scheme, the final occupation number of the controlled state will be different. In those pioneering works on feedback control for achieving ground state [35, 38, 47], a proportional and derivative control is considered. It provides an additional viscous damping of the mechanical oscillator and allows us to achieve a low occupation number. However, such a control scheme is not the optimal one. In order to achieve the minimal occupation number close to zero (quantum ground state), an optimal feedback control is essential. In [41], the optimal controller for general linear quantum dynamics is derived, and the result can be directly applied to the non-Markovian open quantum dynamics of the optomechanical system here. In figure 1, the final occupation number of the unconditional state and optimally controlled state is shown. As long as optimal control is applied, the minimally achievable occupation number of the oscillator will not be constrained by the resolved-sideband limit.

Another interesting issue in the optomechanical system is creating quantum entanglement between the cavity mode and the oscillator, or, even between, two oscillators [3]–[7]. Intuitively, one might think that such an entanglement must be very vulnerable to the thermal decoherence, and the environmental temperature needs to be extremely low in order to create it. However, as shown in [6] and a more recent investigation [53], the environmental temperature—even though an important factor—affects the entanglement implicitly. In [53], an elegant scaling for the entanglement measure is derived and it only depends on the ratio between the strength of optomechanical interaction and that of thermal decoherence. The reason why, in [3]–[5], [7], the

[7] Note that we are focusing on the steady state and therefore the information about the initial quantum state of the mechanical oscillator has decayed away, and the purity of the conditional state will be solely determined by the measurement and optomechanical interaction.

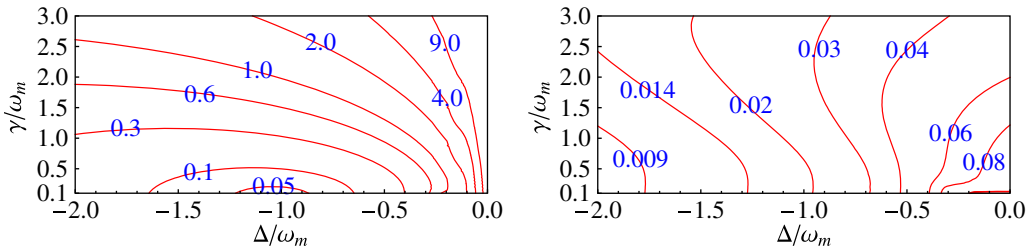

Figure 1. A contour plot of the occupation number as a function of cavity bandwidth γ and detuning Δ for the unconditional state (left) as obtained in [36, 37] and the optimally controlled state (right), the details of which are in sections 3–5.

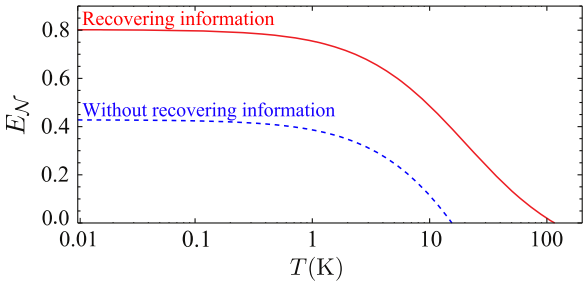

Figure 2. Optomechanical entanglement strength E_N as a function of temperature T with (solid) and without (dashed) recovering information (details are given in section 6).

temperature plays a dominant role in determining the existence of the entanglement can also be traced back to information loss. Here, we will address this issue more explicitly with a rigorous analytical study. Figure 2 shows that, by recovering the information contained in the cavity output, the optomechanical entanglement can even be revived at high temperature. This is a vivid example of a quantum eraser first proposed by Scully and Drühl [54] and later demonstrated experimentally [55]: quantum coherence can be revived by recovering lost information.

The outline of this paper is as follows. In section 2, we will analyze the system dynamics by applying the standard Langevin equation approach and derive the spectral densities of important dynamical quantities. In section 3, we will obtain the unconditional variances of the oscillator position and momentum, and evaluate the corresponding occupation number, which recovers the resolved-sideband limit. In section 4, the conditional variances will be derived via the Wiener-filter approach, which clearly demonstrates that the conditional quantum state is almost pure. In section 5, we will show the occupation number of the optimally controlled state and the corresponding optimal controller to achieve it. In section 6, we will consider the optomechanical entanglement and demonstrate that significant enhancements in the entanglement strength can be achieved after recovering information. In section 7, to motivate cavity-assisted cooling experiments, we will consider imperfections in a real experiment and provide a numerical estimate given a set of experimentally achievable specification. Finally, we will conclude in section 8.

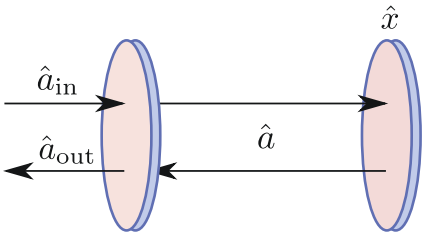

Figure 3. A schematic plot of an optomechanical system with a mechanical oscillator (with displacement $\hat{x}$) coupled to a cavity mode $\hat{a}$, which in turn couples to the external ingoing $\hat{a}_{\rm in}$ and outgoing optical field $\hat{a}_{\rm out}$.

2. Dynamics and spectral densities

In this section, we will analyze the optomechanical dynamics and derive spectral densities of relevant quantities that are essential for obtaining the occupation number of the mechanical oscillator.

2.1. Dynamics

Even though the dynamics of such a system have been discussed extensively in the literature [36, 37, 40], we will go through some equations for the coherence of the present paper. An optomechanical system and the relevant dynamical quantities are shown schematically in figure 3. The corresponding Hamiltonian is given by

$$\hat{\mathcal{H}} = \hbar\omega_{\rm c}\,\hat{a}^\dagger\hat{a} + \frac{\hat{p}^2}{2m} + \frac{1}{2}m\omega_m^2\hat{x}^2 + \hbar G_0\hat{x}\,\hat{a}^\dagger\hat{a} + {\rm i}\hbar\sqrt{2\gamma}\,(\hat{a}_{\rm in}{\rm e}^{-{\rm i}\omega_0 t}\hat{a}^\dagger - {\rm H.c.}). \tag{1}$$

Here, $\omega_{\rm c}$ and ω_0 are the cavity resonant frequency and the laser frequency, respectively; $\hat{a}$ is the annihilation operator for the cavity mode, which satisfies $[\hat{a},\ \hat{a}^\dagger] = 1$; $\hat{x}$ and $\hat{p}$ denote the oscillator position and momentum with $[\hat{x},\ \hat{p}] = {\rm i}\,\hbar$; m is the mass of the oscillator; $G_0 \equiv \omega_0/L$ is the optomechanical coupling constant, with L being the cavity length. In the rotating frame at the laser frequency ω_0, the following nonlinear Langevin equations can be obtained,

$$\dot{\hat{x}}(t) = \hat{p}(t)/m, \tag{2}$$

$$\dot{\hat{p}}(t) = -\gamma_m\hat{p}(t) - m\omega_m^2\hat{x}(t) - \hbar G_0\hat{a}^\dagger(t)\hat{a}(t) + \hat{\xi}_{\rm th}(t), \tag{3}$$

$$\dot{\hat{a}}(t) = -(\gamma - {\rm i}\Delta)\hat{a}(t) - {\rm i}\,G_0\hat{x}(t)\hat{a}(t) + \sqrt{2\gamma}\,\hat{a}_{\rm in}(t), \tag{4}$$

where the cavity detuning $\Delta \equiv \omega_0 - \omega_{\rm c}$. To take into account the fluctuation-dissipation mechanism of the oscillator coupled to a thermal heat bath at temperature T, we have included the mechanical damping γ_m and the associated Brownian force $\hat{\xi}_{\rm th}$, of which the correlation function is $\langle\hat{\xi}_{\rm th}(t)\hat{\xi}_{\rm th}(t')\rangle = 2m\gamma_m k_{\rm B}T\delta(t-t')$ in the high temperature limit. In the cooling experiment, the cavity mode is driven by a coherent laser and, to a good approximation, the system dynamics are linear. To linearize the system, we simply need to replace any operator $\hat{o}(t)$ with the sum of a steady-state part and a small perturbed part, namely $\hat{o}(t) \to \bar{o} + \hat{o}(t)$.[8] We

[8] For simplicity, we use the same $\hat{o}$ to denote its perturbed part.

assume that the mean position of the oscillator is equal to zero with $\bar{x} = 0$. The solution to $\bar{a}$ is given by $\bar{a} = \sqrt{2\gamma}\,\bar{a}_{\rm in}/(\gamma - {\rm i}\Delta)$ and $\bar{a}_{\rm in} = \sqrt{I_0/(\hbar\omega_0)}$, with I_0 being the input optical power. We have chosen an appropriate phase reference such that $\bar{a}$ is real and positive. The resulting linearized equations are

$$m[\ddot{\hat{x}}(t) + \gamma_m \dot{\hat{x}}(t) + \omega_m^2 \hat{x}(t)] = -\hbar\,\bar{G}_0[\hat{a}^\dagger(t) + \hat{a}(t)] + \hat{\xi}_{\rm th}(t), \tag{5}$$

$$\dot{\hat{a}}(t) + (\gamma - {\rm i}\Delta)\hat{a}(t) = -{\rm i}\bar{G}_0\hat{x}(t) + \sqrt{2\gamma}\,\hat{a}_{\rm in}(t), \tag{6}$$

with $\bar{G}_0 \equiv G_0\bar{a}$. The input–output relation of the cavity, which relates the cavity mode to the external continuum optical mode, reads [48]

$$\hat{a}_{\rm out}(t) = \sqrt{\eta}[-\hat{a}_{\rm in}(t) + \sqrt{2\gamma}\,\hat{a}(t)] + \sqrt{1-\eta}\,\hat{n}(t), \tag{7}$$

where η quantifies the quantum efficiency of the photodetector ($\eta = 1$ for a perfect detector) and $\hat{n}$ is the associated vacuum fluctuation that is not correlated with $\hat{a}_{\rm in}$. The linearized dynamics of this system are fully described by equations (5)–(7), which can be solved in the frequency domain.

2.1.1. Mechanical oscillator part. By denoting the Fourier component of any quantity $\hat{O}(t)$ as $\tilde{O}(\Omega)$, the solution to the oscillator position is then

$$\tilde{x}(\Omega) = \tilde{R}_{\rm eff}(\Omega)[\tilde{F}_{\rm BA}(\Omega) + \tilde{\xi}_{\rm th}(\Omega)]. \tag{8}$$

Here, the back-action force $\tilde{F}_{\rm BA}(\Omega)$ is

$$\tilde{F}_{\rm BA}(\Omega) = 2\hbar\bar{G}_0\sqrt{\gamma}\,\chi(\Omega)[(\gamma - {\rm i}\Omega)\tilde{v}_1(\Omega) - \Delta\,\tilde{v}_2(\Omega)], \tag{9}$$

where we have defined the amplitude quadrature $\tilde{v}_1(\Omega)$ and the phase quadrature $\tilde{v}_2(\Omega)$ of the vacuum fluctuation, namely $\tilde{v}_1(\Omega) \equiv [\tilde{a}_{\rm in}(\Omega) + \tilde{a}_{\rm in}^\dagger(-\Omega)]/\sqrt{2}$ and $\tilde{v}_2(\Omega) \equiv [\tilde{a}_{\rm in}(\Omega) - \tilde{a}_{\rm in}^\dagger(-\Omega)]/({\rm i}\sqrt{2})$. Due to the position dependence of the radiation pressure (cf equations (5) and (6)), it gives rise to the well-known optical-spring effect, which modifies the mechanical response of the oscillator from its original value $\tilde{R}_{xx}(\Omega) = -[m(\Omega^2 + 2{\rm i}\gamma_m\Omega - \omega_m^2)]^{-1}$ to an effective one given by

$$\tilde{R}_{\rm eff}(\Omega) \equiv [\tilde{R}_{xx}^{-1}(\Omega) - \tilde{\Gamma}(\Omega)]^{-1}, \tag{10}$$

with $\tilde{\Gamma}(\Omega) \equiv 2\hbar\bar{G}_0^2\,\Delta\,\chi(\Omega)$ and $\chi(\Omega) \equiv [(\Omega + \Delta + {\rm i}\gamma)(\Omega - \Delta + {\rm i}\gamma)]^{-1}$.

2.1.2. Cavity mode part. The solution to the cavity mode is

$$\tilde{a}(\Omega) = \frac{\bar{G}_0\,\tilde{x}(\Omega) + {\rm i}\sqrt{2\gamma}\,\tilde{a}_{\rm in}(\Omega)}{\Omega + \Delta + {\rm i}\gamma}. \tag{11}$$

In terms of amplitude and phase quadratures, it can be rewritten as

$$\tilde{a}_1(\Omega) = \sqrt{2\gamma}\,\chi[(-\gamma + {\rm i}\Omega)\tilde{v}_1(\Omega) + \Delta\,\tilde{v}_2(\Omega)] - \sqrt{2}\,\bar{G}_0\,\Delta\,\chi\,\tilde{x}(\Omega), \tag{12}$$

$$\tilde{a}_2(\Omega) = \sqrt{2\gamma}\,\chi[-\Delta\,\tilde{v}_1(\Omega) - (\gamma - {\rm i}\Omega)\tilde{v}_2(\Omega)] + \sqrt{2}\,\bar{G}_0\,(\gamma - {\rm i}\Omega)\,\chi\,\tilde{x}(\Omega). \tag{13}$$

2.1.3. Cavity output part. Similarly, we introduce amplitude and phase quadratures for the cavity output: $\tilde{Y}_1(\Omega) \equiv [\tilde{a}_{\rm out}(\Omega) + \tilde{a}^\dagger_{\rm out}(-\Omega)]/2$ and $\tilde{Y}_2(\Omega) \equiv [\tilde{a}_{\rm out}(\Omega) - \tilde{a}^\dagger_{\rm out}(-\Omega)]/2$. Their solutions are

$$\tilde{Y}_i(\Omega) = \tilde{Y}_i^{\rm vac}(\Omega) + \sqrt{\eta}\,\tilde{R}_{Y_i F}(\Omega)\,\tilde{x}(\Omega) \quad (i = 1, 2). \tag{14}$$

The vacuum parts $\tilde{Y}_i^{\rm vac}$ of the output, which induce measurement shot noise, are

$$\tilde{Y}_1^{\rm vac}(\Omega) = \sqrt{1-\eta}\,\tilde{n}_1(\Omega) + \sqrt{\eta}\,\chi(\Omega)[(\Delta^2 - \gamma^2 - \Omega^2)\tilde{v}_1(\Omega) + 2\,\gamma\,\Delta\,\tilde{v}_2(\Omega)], \tag{15}$$

$$\tilde{Y}_2^{\rm vac}(\Omega) = \sqrt{1-\eta}\,\tilde{n}_2(\Omega) + \sqrt{\eta}\,\chi(\Omega)[-2\,\gamma\,\Delta\,\tilde{v}_1(\Omega) + (\Delta^2 - \gamma^2 - \Omega^2)\tilde{v}_2(\Omega)]. \tag{16}$$

The output response $\tilde{R}_{Y_i F}(\Omega)$ is defined as [61]

$$\tilde{R}_{Y_1 F}(\Omega) \equiv -2\sqrt{\gamma}\,\bar{G}_0\,\Delta\chi(\Omega), \qquad \tilde{R}_{Y_2 F}(\Omega) \equiv 2\sqrt{\gamma}\,\bar{G}_0(\gamma - {\rm i}\Omega)\chi(\Omega). \tag{17}$$

2.2. Spectral densities

Given the above solutions, we can analyze the statistical properties of the dynamical quantities. We assume all noises to be Gaussian and stationary but not necessarily Markovian, which properly describes the situation in an actual experiment. Their statistical properties are fully quantified by the spectral densities. We define a symmetrized single-sided spectral density $\tilde{S}_{AB}(\Omega)$ according to the standard formula ([62] and references therein)

$$2\pi\,\delta(\Omega - \Omega')\tilde{S}_{AB}(\Omega) = \langle A(\Omega)\tilde{B}^\dagger(\Omega')\rangle_{\rm sym} = \langle \tilde{A}(\Omega)\tilde{B}^\dagger(\Omega') + \tilde{B}^\dagger(\Omega')\tilde{A}(\Omega)\rangle. \tag{18}$$

For vacuum fluctuations $\hat{a}_{1,2}$, we simply have $\tilde{S}_{a_1a_1}(\Omega) = \tilde{S}_{a_2a_2}(\Omega) = 1$ and $\tilde{S}_{a_1a_2}(\Omega) = 0$.

2.2.1. Mechanical oscillator part. The spectral density for the oscillator position is (cf equations (8) and (9))

$$\tilde{S}_{xx}(\Omega) = |\tilde{R}_{\rm eff}(\Omega)|^2\,\tilde{S}^{\rm tot}_{FF}(\Omega), \tag{19}$$

with the noise spectrum for the total force noise given by

$$\tilde{S}_{FF}(\Omega) = 4\hbar m\Omega_q^3\,\gamma\,|\chi(\Omega)|^2(\gamma^2 + \Omega^2 + \Delta^2) + 2\hbar m\Omega_F^2, \tag{20}$$

where we have introduced characteristic frequencies for the optomechanical interaction $\Omega_q \equiv (\hbar\bar{G}_0^2/m)^{1/3}$ and the thermal noise $\Omega_F \equiv \sqrt{2\gamma_m k_{\rm B}T/\hbar}$. The spectral density for the oscillator momentum is simply $\tilde{S}_{pp}(\Omega) = m^2\,\Omega^2\tilde{S}_{xx}(\Omega)$.

2.2.2. Cavity mode part. The spectral density for the cavity mode is a little bit complicated, and it reads

$$\mathbf{S}_{aa}(\Omega) = \mathbf{M}_0\mathbf{M}_0^\dagger + \mathbf{M}_0\mathbf{M}_1^\dagger + \mathbf{M}_1\mathbf{M}_0^\dagger + \mathbf{M}_2\tilde{S}_{xx}(\Omega). \tag{21}$$

Here, elements of the matrix $\mathbf{S}_{aa}$ are denoted by $\tilde{S}_{a_ia_j}(\Omega)$ $(i, j = 1, 2)$; the matrix $\mathbf{M}_0$ is

$$\mathbf{M}_0 \equiv \sqrt{2\gamma}\,\chi(\Omega)\begin{bmatrix} -\gamma + {\rm i}\Omega & \Delta \\ -\Delta & -\gamma + {\rm i}\Omega \end{bmatrix}, \tag{22}$$

the matrix $\mathbf{M}_1$ is

$$\mathbf{M}_1 \equiv 2\sqrt{2\hbar}\bar{G}_0^2\sqrt{\gamma}|\chi(\Omega)|^2\tilde{R}_{\rm eff}(\Omega)\begin{bmatrix} -\Delta(\gamma - {\rm i}\Omega) & \Delta^2 \\ (\gamma - {\rm i}\Omega)^2 & -\Delta(\gamma - {\rm i}\Omega) \end{bmatrix} \tag{23}$$

and the matrix $\mathbf{M}_2$ is

$$\mathbf{M}_2 \equiv 2\bar{G}_0^2|\chi(\Omega)|^2 \begin{bmatrix} \Delta^2 & -\Delta(\gamma+\mathrm{i}\Omega) \\ -\Delta(\gamma-\mathrm{i}\Omega) & \gamma^2+\Omega^2 \end{bmatrix}. \tag{24}$$

The cross correlations between the cavity mode and the output $[\mathbf{S}_{aY}]_{ij} \equiv \tilde{S}_{a_i Y_j}(\Omega)$ are given by

$$\mathbf{S}_{aY} = \mathbf{M}_0\mathbf{M}_3^\dagger + \mathbf{M}_0\mathbf{M}_1^\dagger + \mathbf{M}_1\mathbf{M}_3^\dagger + \sqrt{2\gamma}\mathbf{M}_2\,\tilde{S}_{xx}(\Omega), \tag{25}$$

with

$$\mathbf{M}_3 \equiv \begin{bmatrix} \Delta^2-\gamma^2-\Omega^2 & 2\gamma\Delta \\ -2\gamma\Delta & \Delta^2-\gamma^2-\Omega^2 \end{bmatrix}. \tag{26}$$

The cross correlation between the cavity mode and the oscillator position is

$$\begin{bmatrix} \tilde{S}_{a_1 x}(\Omega) \\ \tilde{S}_{a_2 x}(\Omega) \end{bmatrix} = 2\hbar\bar{G}_0\sqrt{\gamma}\chi^*\tilde{R}^*_{\mathrm{eff}}(\Omega)\mathbf{M}_0 \begin{bmatrix} \gamma+\mathrm{i}\Omega \\ -\Delta \end{bmatrix} + \sqrt{2}\bar{G}_0\chi \begin{bmatrix} -\Delta \\ \gamma-\mathrm{i}\Omega \end{bmatrix} \tilde{S}_{xx}(\Omega). \tag{27}$$

For the oscillator momentum, $\tilde{S}_{a_k p}(\Omega) = \mathrm{i}\,m\Omega\,\tilde{S}_{a_k x}$ $(k = 1, 2)$.

2.2.3. Cavity output part. As an important feature of the quantum noise in this optomechanical system, there is a non-vanishing correlation between the shot noise $\hat{Y}_i^{\mathrm{vac}}$ and the quantum back-action noise $\hat{F}_{\mathrm{BA}}$, and it has the following spectral densities (cf. equations (9), (15) and (16)),

$$\tilde{S}_{FY_1^{\mathrm{vac}}}(\Omega) = 2\sqrt{\hbar m\gamma\eta\Omega_q^3}\,(\gamma+\mathrm{i}\Omega)\,\chi(\Omega)^*, \tag{28}$$

$$\tilde{S}_{FY_2^{\mathrm{vac}}}(\Omega) = 2\sqrt{\hbar m\gamma\eta\Omega_q^3}\,\Delta\,\chi(\Omega)^*, \tag{29}$$

with χ^* being the complex conjugate of χ. Correspondingly, the spectral densities for the output quadratures read

$$\begin{aligned}\tilde{S}_{Y_iY_j}(\Omega) = \delta_{ij} &+ \eta\,\tilde{R}_{Y_iF}(\Omega)\tilde{R}^{\mathrm{eff}}_{xx}(\Omega)\tilde{S}_{FY_j^{\mathrm{vac}}}(\Omega) + \eta[\tilde{R}_{Y_jF}(\Omega)\tilde{R}^{\mathrm{eff}}_{xx}(\Omega)\tilde{S}_{FY_i^{\mathrm{vac}}}(\Omega)]^* \\ &+\eta\,\tilde{R}_{Y_iF}(\Omega)\tilde{R}^*_{Y_jF}(\Omega)\tilde{S}_{xx}(\Omega).\end{aligned} \tag{30}$$

The information about the oscillator position $\hat{x}$ contained in the cavity output $\hat{Y}_i$ are quantified by the cross correlations between $\hat{x}$ and $\hat{Y}_i$, which are

$$\tilde{S}_{xY_i}(\Omega) = \sqrt{\eta}\,\tilde{R}^{\mathrm{eff}}_{xx}(\Omega)\tilde{S}_{FY_i^{\mathrm{vac}}}(\Omega) + \sqrt{\eta}\,\tilde{R}^*_{Y_iF}(\Omega)\tilde{S}_{xx}(\Omega). \tag{31}$$

Similarly, for the oscillator momentum, $\tilde{S}_{pY_k}(\Omega) = -\mathrm{i}\,m\,\Omega\,\tilde{S}_{xY_k}(\Omega)$ $(k = 1, 2)$.

3. Unconditional quantum state and the resolved-sideband limit

In the red-detuned regime ($\Delta < 0$), where those cavity-assisted cooling experiments are currently working, a delayed response of the cavity mode to the oscillator motion gives rise to a viscous damping that can significantly reduce the thermal occupation number of the oscillator, as shown schematically in figure 4. Physically, it acts like a feedback and the mechanical response is changed into an effective one (cf equation (10)), while the thermal force spectrum remains the same. The ground state can be achieved when the occupation number is much

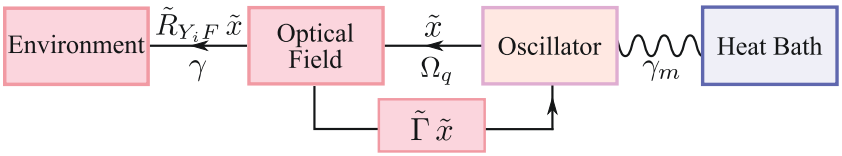

Figure 4. A block diagram of the optomechanical system. The optomechanical cooling can be viewed as a feedback mechanism and reduces the thermal occupation number of the oscillator, which has an effective temperature much lower than the heat bath. Meanwhile, some information about the oscillator motion flows into the environment without being properly treated, leading to the resolved-sideband limit.

smaller than one. If we neglect the information about the oscillator motion that is contained in the output, the resulting quantum state of the oscillator will be *unconditional* and the corresponding occupation number of the oscillator can be obtained with the following standard definition,

$$\mathcal{N} \equiv \frac{1}{\hbar\omega_m}\left(\frac{V_{pp}}{2m} + \frac{1}{2}m\omega_m^2 V_{xx}\right) - \frac{1}{2}, \tag{32}$$

where variances in the oscillator position V_{xx} and momentum V_{pp} are related to the spectral densities by the following formula,

$$V_{xx,pp} = \int_0^\infty \frac{\mathrm{d}\Omega}{2\pi}\,\tilde{S}_{xx,pp}(\Omega). \tag{33}$$

Since $\mathcal{N}$ is dimensionless, it only depends on the following ratios,

$$\Omega_q/\omega_m, \quad \gamma/\omega_m, \quad \Delta/\omega_m, \quad \Omega_F/\omega_m, \quad \gamma_m/\omega_m. \tag{34}$$

The mass and mechanical frequency of the oscillator only enter implicitly. As long as these ratios are the same in different experiments, the final achievable occupation number of different oscillators will be identical.

The resulting $\mathcal{N}$ is shown in the left panel of figure 1. To highlight the quantum limit, we have fixed the interaction strength Ω_q with $\Omega_q/\omega_m = 0.5$, and we have neglected the thermal force noise. In the optimal cooling regime with $\Delta = -\omega_m$, a simple closed form for the occupation number can be obtained [40],

$$\mathcal{N} = \gamma^2/(2\omega_m)^2 + \frac{[1+(\gamma/\omega_m)^2](\Omega_q/\omega_m)^3}{4[1+(\gamma/\omega_m)^2 - 2(\Omega_q/\omega_m)^3)]}. \tag{35}$$

The resolved-sideband limit is achieved for a weak interaction strength $\Omega_q \to 0$ and

$$\mathcal{N}_{\mathrm{lim}} = \gamma^2/(2\omega_m)^2. \tag{36}$$

In the next section, we will demonstrate that such a limit can indeed be surpassed by recovering the information contained in the cavity output.

4. Conditional quantum state and Wiener filtering

Since, given a finite cavity bandwidth, the cavity output contains the information about the oscillator position (cf equation (31)), according to the quantum mechanics, measurements of the

output will collapse the oscillator wave function and project it into a *conditional* quantum state that is in accord with the measurement result. The conditional state, or equivalently its Wigner function, is completely determined by the conditional mean $[x^{\rm cond},\ p^{\rm cond}]$ and the covariance matrix $\mathbf{V}^{\rm cond}$ between the position and momentum. More explicitly, the Wigner function reads

$$W(x,\,p)=\frac{1}{2\pi\sqrt{\det\mathbf{V}^{\rm cond}}}\exp\left[-\frac{1}{2}\delta\vec{X}\,\mathbf{V}^{\rm cond\,-1}\delta\vec{X}^{\rm T}\right], \tag{37}$$

with $\delta\vec{X}=[x-x^{\rm cond},\ p-p^{\rm cond}]$. Since more information is acquired, the conditional quantum state is always more pure than the unconditional counterpart. In the limiting case of an ideal measurement, the conditional quantum state of the mechanical oscillator would be pure with variances constrained by the *Heisenberg uncertainty*, i.e. the determinant of $\mathbf{V}^{\rm cond}$ satisfying $\det\mathbf{V}^{\rm cond}|_{\rm pure\ state}=\hbar^2/4$.

To derive the conditional mean and variances, the usually applied mathematical tool is the SME, which is most convenient for treating Markovian processes [47]–[51]. In the case considered here, however, the cavity has a bandwidth comparable to the mechanical frequency, and the quantum noise is non-Markovian. The corresponding conditional mean and variance can be derived more easily with the Wiener-filtering approach. As shown in [52], the conditional mean of any quantity $\hat{o}(t)$ given a certain measurement result $Y(t')$ $(t<t')$ can be written as

$$o(t)^{\rm cond}\equiv\langle\hat{o}(t)\rangle^{\rm cond}=\int_{-\infty}^{t}{\rm d}t'\,K_{\rm o}(t-t')Y(t'). \tag{38}$$

Here, $K_{\rm o}(t)$ is the optimal Wiener filter and is derived by using the standard Wiener–Hopf method[9]. Its frequency representation is

$$\tilde{K}_{\rm o}(\Omega)=\frac{1}{\tilde{\psi}_{+}(\Omega)}\left[\frac{\tilde{S}_{{\rm o}Y}(\Omega)}{\tilde{\psi}_{-}(\Omega)}\right]_{+}\equiv\frac{\tilde{G}_{\rm o}(\Omega)}{\tilde{\psi}_{+}(\Omega)}, \tag{39}$$

where $[\,]_{+}$ means taking the causal component and $\tilde{\psi}_{\pm}$ is a spectral factorization of the output $\tilde{S}_{YY}\equiv\tilde{\psi}_{+}\tilde{\psi}_{-}$ with $\tilde{\psi}_{+}$ $(\tilde{\psi}_{+})$ and its inverse analytical in the upper-half (lower-half) complex plane and we have introduced $\tilde{G}_{\rm o}(\Omega)$. The conditional covariance between $\hat{A}$ and $\hat{B}$ is given by

$$\begin{aligned}V_{AB}^{\rm cond}&\equiv\langle\hat{A}(t)\hat{B}(t)\rangle_{\rm sym}^{\rm cond}-\langle\hat{A}(t)\rangle^{\rm cond}\langle\hat{B}(t)\rangle^{\rm cond}\\&=\int_{0}^{\infty}\frac{{\rm d}\Omega}{2\pi}[\tilde{S}_{AB}(\Omega)-\tilde{G}_{A}(\Omega)\tilde{G}_{B}^{*}(\Omega)],\end{aligned} \tag{40}$$

where the argument t is eliminated due to stationarity. Since the first term gives the unconditional variance, the second term can be interpreted as a reduction in the uncertainty due to acquiring additional information from the measurement.

These results can be applied directly to the optomechanical system. Suppose we measure the following quadrature of the cavity output,

$$\hat{Y}_{\zeta}=\hat{Y}_{1}\sin\zeta+\hat{Y}_{2}\cos\zeta. \tag{41}$$

Its spectral density reads

$$\tilde{S}_{YY}(\Omega)=\tilde{S}_{Y_1Y_1}(\Omega)\sin^2\zeta+\Re[\tilde{S}_{Y_1Y_2}(\Omega)]\sin(2\zeta)+\tilde{S}_{Y_2Y_2}(\Omega)\cos^2\zeta. \tag{42}$$

[9] For more technical details, one can refer to [52] or the appendix of [65].

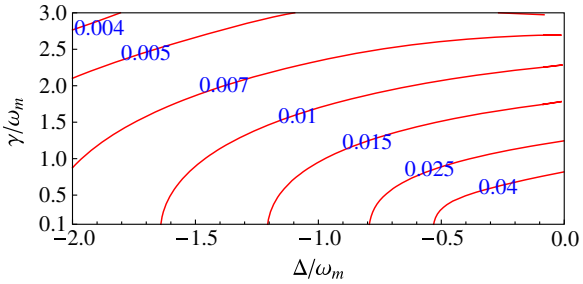

Figure 5. A contour plot of the effective occupation number of the conditional quantum state. For comparison, we have chosen the same specification as in the unconditional case.

The cross correlation between $\hat{Y}_\zeta$ and the oscillator position (momentum) is simply

$$\tilde{S}_{xY,pY} = \tilde{S}_{xY_1,pY_1}(\Omega)\sin\zeta + \tilde{S}_{xY_2,pY_2}(\Omega)\cos\zeta. \tag{43}$$

Substituting the spectral densities $\tilde{S}_{Y_iY_j}$, $\tilde{S}_{xY_i,pY_i}$ and $\tilde{S}_{xx,pp}$ derived in section 2.2 into equation (40), we can obtain the conditional covariances of the oscillator position and momentum, namely $V_{xx}^{\rm cond}$, $V_{pp}^{\rm cond}$ and $V_{xp}^{\rm cond}$.

To quantify how pure the conditional quantum state is, the occupation number defined in equation (32) is no longer an adequate summarizing figure. This is because, generally, $V_{xp}^{\rm cond}$ is not equal to zero, and a pure squeezed state can have a large occupation number defined in equation (32). A well-defined figure of merit is the *uncertainty product*, which is given by

$$U \equiv \frac{2}{\hbar}\sqrt{V_{xx}^{\rm cond}V_{pp}^{\rm cond} - V_{xp}^{\rm cond\,2}}. \tag{44}$$

From it, we can introduce an effective occupation number,

$$\mathcal{N}_{\rm eff} = (U-1)/2, \tag{45}$$

which quantifies how far the quantum state deviates from the pure one ($\mathcal{N}_{\rm eff}=0$). This is identical to the previous definition (cf equation (32)) in the limiting case of $V_{xx}^{\rm cond} = V_{pp}^{\rm cond}/(m^2\omega_m^2)$ and $V_{xp}^{\rm cond}=0$, which is actually satisfied for most of the parameter regimes plotted in figure 1.

For a numerical estimate and a comparison with the unconditional quantum state in the previous section, we assume the same specification and an ideal phase quadrature detection with $\zeta=0$ and $\eta=1$. The resulting effective occupation number is shown in figure 5. Just as expected, the conditional quantum state is not constrained by the resolved-sideband limit and is almost independent of detailed specifications of γ and Δ. The residue occupation number or impurity of the state, shown in figure 5, is due to information about the oscillator motion being confined inside the cavity. Such a confinement is actually attributable to the quantum entanglement between the cavity mode and the oscillator, as we will discuss in section 6.

5. Optimal feedback control

Even though the conditional quantum state has minimum variances in position and momentum, the oscillator itself actually wanders around in the phase space with its center given by the conditional mean $[x^{\rm cond}(t),\ p^{\rm cond}(t)]$ at any instant t. In order to localize the mechanical

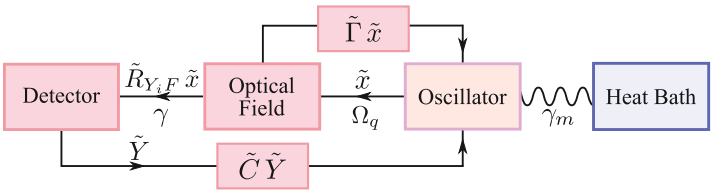

Figure 6. A block diagram for the feedback control scheme. A force is applied onto the mechanical oscillator based on the measurement result with a control kernel $\tilde{C}$. In the detuned case ($\Delta \neq 0$), the radiation pressure and the control force work together to place the mechanical oscillator near its quantum ground state.

oscillator (make the mean position and momentum equal to zero) and achieve its ground state, we need to apply a feedback control, i.e. a force on the oscillator, according to the measurement result. Such a procedure is shown schematically in figure 6. Depending on the choice of the controller, the resulting controlled state will have different occupation numbers. The minimum occupation number can only be achieved if the unique optimal controller is applied. In [41], the optimal controller was derived for a general linear continuous measurement. We will apply the results to this optomechanical system.

Specifically, given the measured output quadrature $\hat{Y}_\zeta$, the feedback force applied to the oscillator can be written in the time domain and the frequency domain as

$$\hat{F}_{\rm FB}(t) = \int_{-\infty}^{t} {\rm d}t'\, C(t-t')\hat{Y}_\zeta(t') \quad \text{and} \quad \tilde{F}_{\rm FB}(\Omega) = \tilde{C}(\Omega)\tilde{Y}_\zeta(\Omega), \tag{46}$$

with $C(t)$ being a causal control kernel. The dynamics of the oscillator will be modified (cf equation (6)) and the new equation of motion of the oscillator reads

$$m[\ddot{\hat{x}}_{\rm ctrl}(t) + \gamma_m \dot{\hat{x}}_{\rm ctrl}(t) + \omega_m^2 \hat{x}_{\rm ctrl}(t)] = -\hbar\, \bar{G}_0[\hat{a}^\dagger(t) + \hat{a}(t)] + \hat{\xi}_{\rm th}(t) + \hat{F}_{\rm FB}(t). \tag{47}$$

In the frequency domain, the controlled oscillator position $\hat{x}_{\rm ctrl}$ is related to the uncontrolled one $\hat{x}$ by

$$\tilde{x}_{\rm ctrl}(\Omega) = \tilde{x}(\Omega) + \frac{\tilde{R}^{\rm eff}_{xx}(\Omega)\tilde{C}(\Omega)\tilde{Y}_\zeta(\Omega)}{1 - \tilde{R}^{\rm eff}_{xx}(\Omega)\tilde{R}_{Y_\zeta F}(\Omega)\tilde{C}(\Omega)}. \tag{48}$$

As shown in [41], by minimizing the effective occupation number of the controlled state, the optimal controller can be derived and is given by

$$\tilde{C}^{\rm opt}(\Omega) = -\frac{\tilde{R}^{\rm eff}_{xx}(\Omega)^{-1}\tilde{K}^{\rm opt}_{\rm ctrl}(\Omega)}{1 - \tilde{R}_{YF}(\Omega)\tilde{K}^{\rm opt}_{\rm ctrl}(\Omega)}, \tag{49}$$

where

$$\tilde{K}^{\rm opt}_{\rm ctrl}(\Omega) = \frac{1}{\tilde{\psi}_+(\Omega)}\left[\tilde{G}_x(\Omega) - \frac{G_x(0)}{\sqrt{V^{\rm cond}_{pp}/V^{\rm cond}_{xx}} - {\rm i}\,\Omega}\right], \tag{50}$$

with $\tilde{G}_x(\Omega) = [\tilde{S}_{xY}(\Omega)/\tilde{\psi}_-(\Omega)]_+$ defined in equation (39).

From equation (48), we can find out the spectral densities and the covariance for the controlled position and momentum. As it turns out, there is an intimate connection between the

optimally controlled state and the conditional quantum state. Due to the requirement of stationarity ($V_{xx}^{\rm ctrl}$ and $V_{pp}^{\rm ctrl}$ are constant), it indicates that $V_{xp}^{\rm ctrl}=0$ because $V_{xp}^{\rm ctrl}=(1/2)m\dot{V}_{xx}^{\rm ctrl}=0$, and, therefore, the optimally controlled state is always less pure than the conditional state. The corresponding uncertainty product of the optimally controlled state reads [41]

$$U_{\rm ctrl}^{\rm opt}=\frac{2}{\hbar}\sqrt{V_{xx}^{\rm ctrl}V_{pp}^{\rm ctrl}}|_{\rm optimally\ controlled}=\frac{2}{\hbar}\left[\sqrt{V_{xx}^{\rm cond}V_{pp}^{\rm cond}}+|V_{xp}^{\rm cond}|\right]. \tag{51}$$

The occupation number $\mathcal{N}$ for the optimally controlled state was shown in figure 1 in the introduction. Since $V_{xp}^{\rm cond}$ is quite small compared with $V_{xx,pp}^{\rm cond}$, the resulting occupation number is very close to that of the conditional quantum state. Therefore, as long as the optimal controller is applied, the mechanical oscillator is almost in its quantum ground state and the resolved-sideband limit does not impose significant constraints.

6. Conditional optomechanical entanglement and the quantum eraser

In this section, we will analyze the optomechanical entanglement between the oscillator and the cavity mode. In particular, we will show that (i) the residue impurity of the conditional quantum state of the oscillator is attributable to the optomechanical entanglement and (ii), if the environmental temperature is high, the existence of entanglement critically depends on whether the information in the cavity output is recovered or not. In other words, the quantum correlation is affected by the 'eraser' of certain information, and this manifests the idea of 'quantum eraser' proposed by Scully and Drühl [54], which is well known in the quantum optics community.

The existence of optomechanical entanglement is shown in the pioneering work by Vitali *et al* [4]. The entanglement criterion, i.e. inseparability, is based on the positivity of the partially transposed density matrix [56]–[58]. In the case of Gaussian variables considered here, this reduces to the following uncertainty principle in phase space,

$$\mathbf{V}_{\rm pt}+\frac{1}{2}\mathbf{K}\geqslant 0,\qquad \mathbf{K}=\begin{pmatrix}0 & -2{\rm i}\\ 2{\rm i} & 0\end{pmatrix}, \tag{52}$$

with $\mathbf{K}$ denoting the commutator matrix. The subscript 'pt' is short for partial transpose. The partial transpose transform is equivalent to time reversal. In the phase space, the momentum of the oscillator changes sign, and the corresponding partially transposed covariance matrix $\mathbf{V}_{\rm pt}\equiv\mathbf{V}|_{\hat{p}\to-p}$. From the Williamson theorem, there exists a symplectic transformation $\mathbf{S}\in S_{p(4,\mathbf{R})}$ such that $\mathbf{S}^{\rm T}\mathbf{V}_{\rm pt}\mathbf{S}=\bigoplus_{i=1}^{2}{\rm Diag}[\lambda_i,\ \lambda_i]$. Using the fact that $\mathbf{S}^{\rm T}\mathbf{K}\mathbf{S}=\mathbf{K}$, the above uncertainty principle requires $\lambda_i\geqslant 1$. If $\exists\lambda<1$, the states are entangled. The amount of entanglement can be quantified by the logarithmic negativity $E_{\mathcal{N}}$, which is defined as ([59]; [60] and references therein)

$$E_{\mathcal{N}}\equiv\max[-\ln\lambda,\ 0]. \tag{53}$$

Given a 4×4 covariance matrix $\mathbf{V}$ between the oscillator $[\hat{x},\ \hat{p}]$ and the cavity mode $[\hat{a}_1,\ \hat{a}_2]$, the simplectic eigenvalue λ has the following closed form

$$\lambda=\sqrt{\Sigma-\sqrt{\Sigma^2-4\det\mathbf{V}}}/\sqrt{2}, \tag{54}$$

where $\Sigma\equiv\det\mathbf{A}+\det\mathbf{B}-2\det\mathbf{C}$ and

$$\mathbf{V}=\langle[\hat{x},\ \hat{p},\ \hat{a}_1,\ \hat{a}_2]^T[\hat{x},\ \hat{p},\ \hat{a}_1,\ \hat{a}_2]\rangle_{\rm sym}=\begin{bmatrix}\mathbf{A}_{2\times 2} & \mathbf{C}_{2\times 2}\\ \mathbf{C}_{2\times 2}^{\rm T} & \mathbf{B}_{2\times 2}\end{bmatrix}. \tag{55}$$

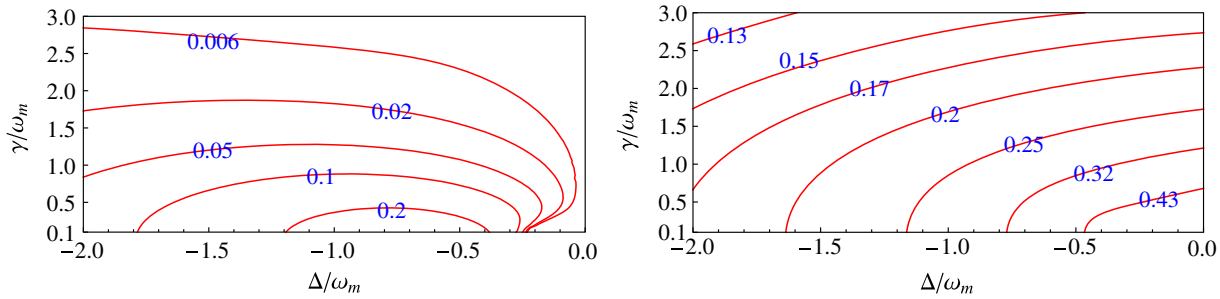

Figure 7. Contour plots of the logarithmic negativity $E_{\mathcal{N}}$ for unconditional (left) and conditional (right) entanglement between the cavity mode and the oscillator. We have assumed that $\Omega_q/\omega_m = 0.5$ to make sure that the resulting optomechanical system is stable in those parameter regimes shown in the figure. In addition, to manifest the entanglement, we have ignored thermal noise.

In [4], the information contained in the cavity output is ignored and unconditional covariances are used to evaluate the entanglement measure $E_{\mathcal{N}}$. We can call it unconditional entanglement. If the information is recovered, conditional covariances obtained in equation (40) will replace the unconditional counterparts. In figure 7, we compare the unconditional and the conditional entanglement, and the figure clearly shows that the entanglement strength increases dramatically in the conditional case. Additionally, the regime where the entanglement is strong is in accord with where the conditional quantum state of the oscillator is less pure, as shown in figure 5. Indeed, there is a simple analytical relation between the effective occupation number $\mathcal{N}_{\rm eff}$ and the logarithmic negativity $E_{\mathcal{N}}$ in this ideal case with no thermal noise—that is,

$$E_{\mathcal{N}} = -2\ln[\sqrt{\mathcal{N}_{\rm eff}+1} - \sqrt{\mathcal{N}_{\rm eff}}] \approx 2\sqrt{\mathcal{N}_{\rm eff}} \tag{56}$$

for small $\mathcal{N}_{\rm eff}$ [59]. Therefore, the quantum limitation of a cooling experiment actually arises from the optomechanical entanglement, which justifies our claim in section 4.

If we take into account the environmental temperature, as shown in figure 2 in the introduction, the unconditional entanglement vanishes when the temperature is higher than 10 K, given the following specifications: $\gamma/\omega_m = 1$, $\Delta/\omega_m = -1$, $\Omega_q/\omega_m = 1$, and the mechanical quality factor $Q_m \equiv \omega_m/\gamma_m = 5 \times 10^5$. In contrast, the conditional one exists even when the temperature rises higher than 100 K. Therefore, only when the information contained in the cavity output is properly treated will the observer be able to recover the quantum correlation between the oscillator and the cavity mode at high temperature. In fact, the temperature is not the only figure that determines the existence of quantum entanglement. A recent investigation showed that, in the simple system with an oscillator interacting with a coherent optical field, quantum entanglement always exists between the oscillator and the outgoing optical field [53]. The resulting entanglement strength only depends on the ratio between the characteristic interaction strength Ω_q and the thermal-noise strength Ω_F, which depends on the environmental temperature. We can make some connections to the results in [53] by assuming a large cavity bandwidth. In such a case, the cavity mode exchanges information with the external outgoing field at a timescale much shorter than the thermal decoherence timescale of the oscillator. In figure 8, we show the resulting $E_{\mathcal{N}}$ of the conditional entanglement as a function of cavity bandwidth and environmental temperature with fixed interaction strength.

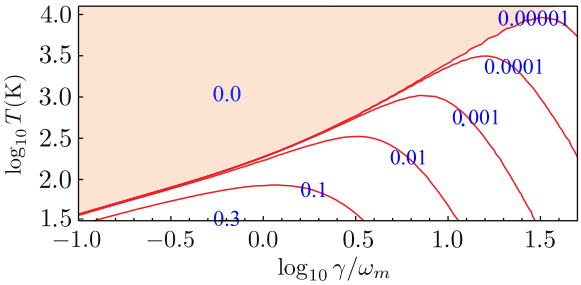

Figure 8. Logarithmic negativity $E_{\mathcal{N}}$ as a function of cavity bandwidth and environmental temperature. We have chosen $\Omega_q/\omega_m = 1$, $\Delta = 0$, $Q_m = 5 \times 10^5$ and $\omega_m/2\pi = 10^6$ Hz. The shaded regimes are where entanglement vanishes.

The entanglement can persist at a very high temperature (10^4 K shown in this plot!) as long as the cavity bandwidth is large. This, to some extent, recovers the results obtained in [53].

7. Experimental realization and numerical estimate

In the following, we will consider the experimental realization of such a scheme by discussing various imperfections that exist in an actual experiment, e.g. the classical laser noise, non-unity quantum efficiency of the photodetector, environmental thermal noise and optical loss.

The classical laser noise has been pointed out to be an important issue by Diosi [42] and more recently by Rabl *et al* [43]. The laser amplitude and phase noises induce both readout noise and stochastic force noise on to the mechanical oscillator, which increases the occupation number. Their effects, in principle, can be reduced by using either the interferometric setup presented in [63] or the three-mode optomechanical interaction [44, 64]. The non-unity quantum efficiency of the photodetector and the environmental thermal noise has already been taken into account in the equations of motion, which induces uncorrelated vacuum fluctuation. Similarly, for the optical loss, some uncorrelated vacuum fields enter the cavity in an unpredictable way. A small optical loss will not modify the cavity bandwidth significantly but will introduce an additional force noise, which is (cf equation (28))

$$S_{FF}^{\mathrm{add}}(\Omega) = 4\hbar m\, \Omega_{\mathrm{q}}^3\, \gamma_\epsilon\, |\chi|^2(\gamma^2 + \Omega^2 + \Delta^2), \tag{57}$$

where $\gamma_\epsilon \equiv c\,\epsilon/(4L)$ is the effective bandwidth that is induced by an optical loss of ϵ.

To motivate table-top cavity-assisted cooling experiments, we will use the following experimental achievable parameters for a numerical estimate,

$$\begin{aligned} &m = 1\,\mathrm{mg}, \quad I_0 = 20\,\mathrm{mW}, \quad \mathcal{F} = 3 \times 10^4, \quad \omega_{\mathrm{m}}/(2\pi) = 10^5\,\mathrm{Hz}, \\ &Q_{\mathrm{m}} = 5 \times 10^6, \quad L = 1\,\mathrm{cm}, \quad \eta = 0.95, \quad \epsilon = 10\,\mathrm{ppm}, \end{aligned} \tag{58}$$

where $\mathcal{F} \equiv \pi c/(L\gamma)$ is the cavity finesse. This gives a coupling strength of $\Omega_q/\omega_m \approx 0.6$ (we have chosen $\Delta = -\omega_m$) and a cavity bandwidth $\gamma/\omega_m = 2.5$. The final results will not change if we increase both the mass and the optical power with the same factor, which essentially gives the same effective interaction strength, and therefore, it can easily be extended to a large-scale experiment with a massive mechanical oscillator. In figure 9, we show the corresponding occupation number for the controlled state as a function of environmental temperature and

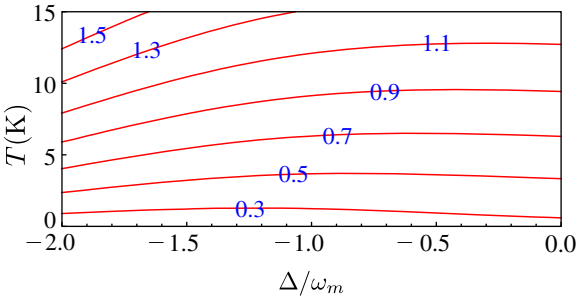

Figure 9. Occupation number of the optimally controlled state as a function of the temperature and the cavity detuning. The other specifications are chosen to be achievable in an actual experiment, which are detailed in the main text.

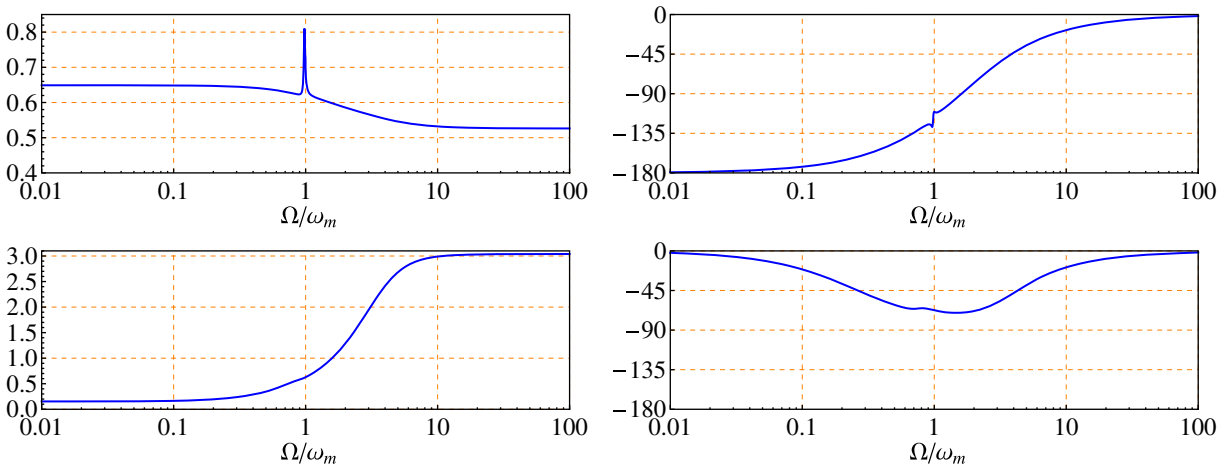

Figure 10. Bode plots of the amplitude (left column) and phase (right column) of control kernels $\tilde{C}(\Omega)$. The first row shows the case of $\Omega_q/\omega_m = 0.6$ and the controller is roughly a notch filter at the mechanical frequency. The second row presents the case of $\Omega_q/\omega_m = 1.2$, and the corresponding controller can be approximately a lead compensator. The other specifications are the same as listed in the main text.

cavity detuning. An occupation number of less than one can be achieved when the environmental temperature falls lower than 10 K given the above specifications. If the oscillator can sustain a higher optical power, one can increase the interaction strength to reduce thermal excitations.

The corresponding feedback control can be realized by using either a capacitive drive or the radiation pressure of another auxiliary laser, as demonstrated in the experiment [13]. The Bode plot of the optimal controller in the particular case with an environmental temperature of 5 K is shown in figure 10. As we can see when the interaction strength (the optical power) increases, the optimal controller is approximately a lead compensator[10],

$$\tilde{C}(\Omega) \approx \alpha_0 \frac{\Omega + \mathrm{i}\,\alpha_1}{\Omega + \mathrm{i}\,\alpha_2}, \tag{59}$$

[10] There is a difference in the sign of the phase due to the definition of Fourier transform: $\tilde{f}(\Omega) = \int \mathrm{d}t f(t) \mathrm{e}^{\mathrm{i}\Omega t}$ rather than $\int \mathrm{d}t f(t) \mathrm{e}^{-\mathrm{i}\Omega t}$.

with α_i $(i = 0, 1, 2)$ being some constants and $\alpha_2 \geqslant \alpha_1$. It is a derivative controller around the mechanical frequency, and this, to some extent, justifies the use of the band-limited derivative controller in the experiment.

We have been discussing the experimental realization of achieving the quantum ground state of the mechanical oscillator. To realize the optomechanical entanglement, the experimental requirement is almost the same as that for achieving the quantum ground state. The subtle issue here is verifying such conditional entanglement. This would require an additional verification stage to obtain the condition covariance matrix $\mathbf{V}$ in equation (55) or equivalently the joint conditional distribution of dynamical variables $[\hat{x}, \hat{p}, \hat{a}_1, \hat{a}_2]$. In general, there will be some added error due to measurement noise during the verification stage. For Gaussian noises, such an error can be quantified by a covariance matrix $\mathbf{V}_{\rm add}$. To reveal the quantum correlation (entanglement), the verification error has to be below the Heisenberg limit—a quantum tomography process[11]. To achieve this, we can apply the experimental verification procedure proposed in [65], where the verification of entanglement between two mechanical oscillators is discussed, and the mathematical structure is entirely the same as what has been considered here. The basic idea is to apply a time-dependent homodyne detection of the cavity output to measure the optical and mechanical quadratures. By optimizing the time-dependent phase of the local oscillator for the homodyne detection, the verification error can be significantly smaller than the Heisenberg limit.

8. Conclusion

We have shown that both the conditional state and the optimally controlled state of the mechanical oscillator can achieve a low occupation number, even if the cavity bandwidth is large. Therefore, as long as the information about the oscillator motion contained in the cavity output is carefully recovered, the resolved-sideband limit will not pose a fundamental limit in cavity-assisted cooling experiments. This work can help us understand the intermediate regime between the optomechanical cooling and feedback cooling, which will be useful for searching optimal parameters for a given experimental setup. In addition, we have shown that the optomechanical entanglement between the cavity mode and the oscillator can be significantly enhanced by recovering information, and its existence becomes insensitive to the environmental temperature.

Acknowledgments

We thank T Corbitt, F Ya Khalili, H Rehbein and our colleagues at TAPIR and the MQM group for fruitful discussions. HM is supported by the Australian Research Council and the Department of Education, Science and Training. SD, HM-E and YC are supported by the Alexander von Humboldt Foundation's Sofja Kovalevskaja program, NSF grants PHY-0653653 and PHY-0601459, as well as the David and Barbara Groce startup fund at Caltech. HM thanks D G Blair, L Ju and C Zhao for their keen support of his visit to Caltech.

[11] If $\mathbf{V}_{\rm add}$ is Heisenberg limited, namely $\mathbf{V}_{\rm add} + \frac{1}{2}\mathbf{K} \geqslant 0$ (cf equation (52)), it follows that $\mathbf{V}_{\rm pt} + \mathbf{V}_{\rm add} + \frac{1}{2}\mathbf{K} > 0$. This indicates that, after the verification stage, there will be no quantum correlation.

References

[1] Braginsky V B and Khalili F Ya 1992 *Quantum Measurement* (Cambridge: Cambridge University Press)
[2] Marshall W, Simon C, Penrose R and Bouwmeester D 2003 *Phys. Rev. Lett.* **90** 130401
[3] Mancini S, Vitali D and Tombesi P 2003 *Phys. Rev. Lett.* **90** 137901
[4] Vitali D, Gigan S, Ferreira A, Böhm H R, Tombesi P, Guerreiro A, Vedral V, Zeilinger A and Aspelmeyer M 2007 *Phys. Rev. Lett.* **98** 030405
[5] Paternostro M, Vitali D, Gigan S, Kim M S, Brukner C, Eisert J and Aspelmeyer M 2007 *Phys. Rev. Lett.* **99** 250401
[6] Müller-Ebhardt H, Rehbein H, Schnabel R, Danzmann K and Chen Y 2008 *Phys. Rev. Lett.* **100** 013601
[7] Hartmann M J and Plenio M B 2008 *Phys. Rev. Lett.* **101** 200503
[8] Zurek W 1981 *Phys. Rev.* D **24** 1516
Zurek W 1982 *Phys. Rev.* D **26** 1862
Zurek W 1991 *Phys. Today* **44** 36
[9] Diósi L 1987 *Phys. Lett.* A **120** 377
Diósi L 1987 *Phys. Rev.* A **40** 1165
Diósi L 2007 *J. Phys. A: Math. Theor.* **40** 2989
[10] Penrose R 1996 *Gen. Rel. Grav.* **28** 581
Penrose R 1996 *Phil. Trans. R. Soc.* A **356** 1927
Penrose R 2005 *The Road to Reality: A Complete Guide to the Laws of the Universe* (New York: Alfred A Knopf)
[11] O'Connell A D *et al* 2010 *Nature* **464** 697–703
[12] Blair D, Ivanov E, Tobar M, Turner P, van Kann F and Heng I 1995 *Phys. Rev. Lett.* **74** 1908
[13] Cohadon P, Heidmann A and Pinard M 1999 *Phys. Rev. Lett.* **83** 3174
[14] Metzger C and Karrai K 2004 *Nature* **432** 1002
[15] Naik A, Buu O, LaHaye M, Armour A D, Clerk A, Blencowe M and Schwab K 2006 *Nature* **443** 14
[16] Gigan S, Böhm H R, Paternostro M, Blaser F, Langer G, Hertzberg J B, Schwab K C, Bäuerle D, Aspelmeyer M and Zeilinger A 2006 *Nature* **444** 67
[17] Arcizet O, Cohandon P, Briant T, Pinard M and Heidmann A 2006 *Nature* **444** 71
[18] Kleckner D and Bouwmeester D 2006 *Nature* **444** 75
[19] Schliesser A, DelHaye P, Nooshi N, Vahala K and Kippenberg T 2006 *Phys. Rev. Lett.* **97** 243905
[20] Corbitt T, Chen Y, Innerhofer E, Muller-Ebhardt H, Ottaway D, Rehbein H, Sigg D, Whitcomb S, Wipf C and Mavalvala N 2007 *Phys. Rev. Lett.* **98** 150802
[21] Corbitt T, Wipf C, Bodiya T, Ottaway D, Sigg D, Smith N, Whitcomb S and Mavalvala N 2007 *Phys. Rev. Lett.* **99** 160801
[22] Schliesser A, Rivire R, Anetsberger G, Arcizet O and Kippenberg T 2008 *Nature Phys.* **4** 415
[23] Poggio M, Degen C L, Mamin H J and Rugar D 2007 *Phys. Rev. Lett.* **99** 017201
[24] Favero I, Metzger C, Camerer S, König D, Lorenz H, Kotthaus J and Karrai K 2007 *Appl. Phys. Lett.* **90** 104101
[25] Teufel J, Harlow J, Regal C and Lehnert K 2008 *Phys. Rev. Lett.* **101** 197203
[26] Thompson J, Zwickl B, Jayich A, Marquardt F, Girvin S and Harris J 2008 *Nature* **452** 72
[27] Mow-Lowry C, Mullavey A, Goßler S, Gray M and McClelland D 2008 *Phys. Rev. Lett.* **100** 010801
[28] Gröblacher S, Gigan S, Böhm H R, Zeilinger A and Aspelmeyer M 2008 *Europhys. Lett.* **81** 54003
[29] Schediwy S W, Zhao C, Ju L, Blair D G and Willems P 2008 *Phys. Rev.* A **77** 013813
[30] Jourdan G, Comin F and Chevrier J 2008 *Phys. Rev. Lett.* **101** 133904
[31] Gröblacher S, Hertzberg J, Vanner M, Cole G, Gigan S, Schwab K and Aspelmeyer M 2009 *Nature Phys.* **5** 485
[32] Abbott B *et al* 2009 LIGO Scientific Collaboration *New J. Phys.* **11** 073032
[33] Rocheleau T, Ndukum T, Macklin C, Hertzberg J, Clerk A and Schwab K 2010 *Nature* **463** 72

[34] Vyatchanin S 1977 *Dokl. Akad. Nauk SSSR* **234** 1295
[35] Mancini S, Vitali D and Tombesi P 1998 *Phys. Rev. Lett.* **80** 688
[36] Marquardt F, Chen J, Clerk A and Girvin S 2007 *Phys. Rev. Lett.* **99** 093902
[37] Wilson-Rae I, Nooshi N, Zwerger W and Kippenberg T 2007 *Phys. Rev. Lett.* **99** 093901
[38] Courty J M, Heidmann A and Pinard M 2001 *Eur. Phys. J.* D **17** 399
[39] Vitali D, Mancini S, Ribichini L and Tombesi P 2002 *Phys. Rev.* A **65** 063803
[40] Genes C, Vitali D, Tombesi P, Gigan S and Aspelmeyer M 2008 *Phys. Rev.* A **77** 033804
[41] Danilishin S, Müller-Ebhardt H, Rehbein H, Somiya K, Schnabel R, Danzmann K, Corbitt T, Wipf C, Mavalvala N and Chen Y 2008 arXiv:0809.2024 [quant-ph]
[42] Diósi L 2008 *Phys. Rev.* A **78** 021801
[43] Rabl P, Genes C, Hammerer K and Aspelmeyer M 2009 *Phys. Rev.* A **80** 063819
[44] Zhao C, Ju L, Miao H, Gras S, Fan Y and Blair D 2009 *Phys. Rev. Lett.* **102** 243902
[45] Elste F, Girvin S and Clerk A 2009 *Phys. Rev. Lett.* **102** 207209
[46] Corbitt T private communication
[47] Hopkins A, Jacobs K, Habib S and Schwab K 2003 *Phys. Rev.* B **68** 235328
[48] Gardiner C and Zoller P 2004 *Quantum Noise* 3rd edn (Berlin: Springer)
[49] Milburn G 1996 *Quantum Semiclass. Opt.* **8** 269
[50] Doherty A, Tan S, Parkins A and Walls D 1999 *Phys. Rev.* A **60** 2380
[51] Doherty A and Jacobs K 1999 *Phys. Rev.* A **60** 2700
[52] Müller-Ebhardt H, Rehbein H, Li C, Mino Y, Somiya K, Schnabel R, Danzmann K and Chen Y 2009 *Phys. Rev.* A **80** 043802
[53] Miao H, Danilishin S and Chen Y 2010 *Phys. Rev.* A **81** 052307
[54] Scully M and Drühl K 1982 *Phys. Rev.* A **25** 2208
[55] Kim Y, Yu R, Kulik S, Shih Y and Scully M 2000 *Phys. Rev. Lett.* **84** 1
[56] Peres A 1996 *Phys. Rev. Lett.* **77** 1413
[57] Horodecki M, Horodecki P and Horodecki R 1996 *Phys. Lett.* A **223** 1
[58] Simon R 2000 *Phys. Rev. Lett.* **84** 2726
[59] Vidal G and Werner R F 2002 *Phys. Rev.* A **65** 032314
[60] Review article by Adesso G and Illuminati F 2007 *J. Phys. A: Math. Theor.* **40** 7821
Horodecki R, Horodecki P, Horodecki M and Hordecki K 2009 *Rev. Mod. Phys.* **81** 865
[61] Buonanno A and Chen Y 2003 *Phys Rev.* D **67** 062002
[62] Kimble H J, Levin Y, Matsko A B, Thorne K S and Vyatchanin S P 2001 *Phys. Rev.* D **65** 022002
[63] Corbitt T, Chen Y, Khalili F, Ottaway D, Vyatchanin S, Whitcomb S and Mavalvala N 2006 *Phys. Rev.* A **73** 023801
[64] Yin Z 2009 *Phys. Rev.* A **80** 033821
[65] Miao H, Danilishin S, Müller-Ebhardt H, Rehbein H, Somiya K and Chen Y 2010 *Phys. Rev.* A **81** 012114